



HAL
open science

Photoactivatable Liposomes for Blue to Deep Red Light-Activated Surface Drug Release: Application to Controlled Delivery of the Antitumoral Drug Melphalan

Anaïs Brion, Juliane Chaud, Maxime Klimezak, Frédéric Bolze, Laura Ohlmann, Jérémie Léonard, Stefan Chassaing, Benoît Frisch, Antoine Kichler, Béatrice Heurtault, et al.

► To cite this version:

Anaïs Brion, Juliane Chaud, Maxime Klimezak, Frédéric Bolze, Laura Ohlmann, et al.. Photoactivatable Liposomes for Blue to Deep Red Light-Activated Surface Drug Release: Application to Controlled Delivery of the Antitumoral Drug Melphalan. *Bioconjugate Chemistry*, 2023, 34 (7), pp.1304-1315. 10.1021/acs.bioconjchem.3c00197 . hal-04154766

HAL Id: hal-04154766

<https://hal.science/hal-04154766v1>

Submitted on 6 Jul 2023

HAL is a multi-disciplinary open access archive for the deposit and dissemination of scientific research documents, whether they are published or not. The documents may come from teaching and research institutions in France or abroad, or from public or private research centers.

L'archive ouverte pluridisciplinaire **HAL**, est destinée au dépôt et à la diffusion de documents scientifiques de niveau recherche, publiés ou non, émanant des établissements d'enseignement et de recherche français ou étrangers, des laboratoires publics ou privés.

Photoactivatable liposomes for blue to deep red light activated surface drug release: application to controlled delivery of the antitumoral drug melphalan

Anaïs Brion^{1#}, Juliane Chaud^{1,2#}, Maxime Klimezak², Frédéric Bolze², Laura Ohlmann¹, Jérémie Léonard³, Stefan Chassaing⁴, Benoît Frisch¹, Antoine Kichler¹, Béatrice Heurtault^{1*}, Alexandre Specht^{2*}

¹ 3Bio Team, Laboratoire de Conception et Application de Molécules Bioactives, UMR 7199 Université de Strasbourg/CNRS, Faculté de Pharmacie, F-67401 Illkirch Cedex.

² Équipe de chimie et neurobiologie moléculaire, Laboratoire de Conception et Application de Molécules Bioactives, UMR 7199 Université de Strasbourg/CNRS, Faculté de Pharmacie, F-67401 Illkirch Cedex.

³ Institut de Physique et Chimie des Matériaux de Strasbourg, Université de Strasbourg/CNRS, UMR 7504, F-67034 Strasbourg.

⁴ Institut de Chimie, Laboratoire de Synthèse, Réactivité Organiques & Catalyse, (LASYROC), Institut de Chimie, UMR 7177 Université de Strasbourg/CNRS, F-67000 Strasbourg.

* Correspondence and requests for materials should be addressed to B.H. (bheurtault@unistra.fr) or A.S. (specht@unistra.fr).

Anaïs Brion and Juliane Chaud contributed equally to this work.

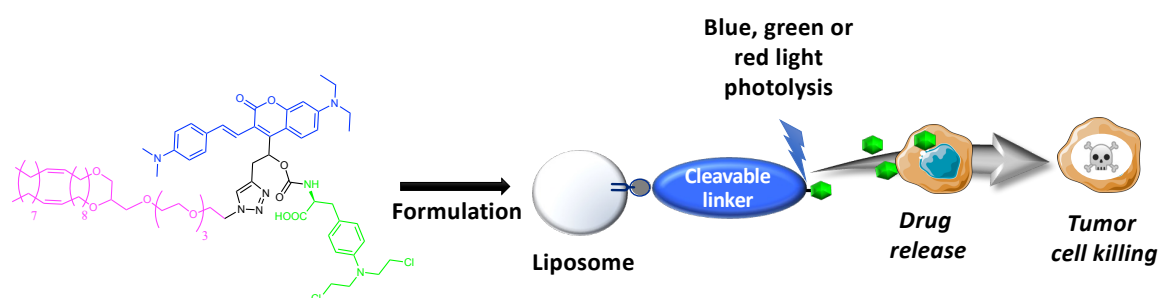
ABSTRACT

Liposome-based nanoparticles able to release, via a photolytic reaction, a payload anchored at the surface of the phospholipid bilayer were prepared. The liposome formulation strategy is using an original drug conjugated blue light sensitive photoactivatable coumarinyl linker. This latter is based on an efficient blue light sensitive photolabile protecting group modified by a lipid anchor which enables its incorporation into liposomes leading to blue to green light sensitive nanoparticles. In addition, formulated liposomes were doped with Triplet-Triplet Annihilation upconverting organic chromophores (red to blue light) in order to prepare red light sensitive liposomes able to release a payload, by upconversion assisted photolysis. Those light-activatable liposomes were used to demonstrate that direct

blue or green light photolysis or red light TTA-UC assisted drug-photolysis can effectively photorelease a drug payload (Melphalan) and kill tumor cells *in vitro* after photoactivation.

KEYWORDS: Liposomes – Photoremovable protecting groups - Prodrug – Drug delivery – Photopharmacology

GRAPHICAL ABSTRACT



INTRODUCTION

Liposomes (Lps) are phospholipid-based single or multi-lamellar bilayer spherical nanoparticles with an aqueous core. Due to their physicochemical properties, such as their colloidal nature, size, ease of preparation and lack of toxicity and immunogenicity, liposomes are widely investigated as delivery vehicles.^{1,2} The bioactive compound that has to be delivered can be either encapsulated into the liposomes (either in the aqueous core or in the lipid bilayers for hydrophobic compounds) or anchored on their surface.³ Due to their versatility, liposomes are the most successful vehicle in nanomedicine, with 14 drugs in clinical use for cancer therapy, fungal infections treatment, analgesics, viral vaccines or photodynamic therapy.⁴

A strategy that could widen the use of those nanoparticles in nanomedicine is the development of liposomes that allow a control of the release of biological effectors using non-invasive stimuli. Such approaches are not only of interest in fundamental science but also in applied science as they could open perspectives for the treatment of acquired and genetic diseases. Indeed, precise spatial and temporal control of the release of the therapeutic agent would allow a coordination for a perfect match between drug availability and disease activity.

For triggering drug release by external stimuli various strategies have been developed, among which light is particularly attractive. Indeed, light exposure can be precisely controlled over the irradiation time and intensity and, as a consequence, the strength of the stimulus can be modulated. In particular, the concept of chemophototherapy^{5,6} which combines photodynamic therapy (PDT) and classical chemotherapy has recently been studied in a large number of preclinical and clinical works. In addition, implantable biocompatible micro light emitting diode (μ LED) devices have been developed to perform noninvasive light stimulations deep in the mouse body.⁷

Photoactivation techniques, generally speaking, including photolysis (photo-triggered release), sensitizer-assisted light-induced redox and photoisomerization, have proved attractive in various fields of chemistry and biology.⁸ Noteworthy, for *in vivo* applications of smart nanocarriers, light-induced content release must be highly efficient and capable of responding to wavelengths that can penetrate into the tissues.⁹⁻¹⁰ Several methods have already been described for light-controlled content release from liposomes.¹¹⁻¹⁷ For biomedical applications the use of photolytic reactions looks very attractive for a fine controlled drug release by light. Light controlled drug release has been achieved with photoremovable groups or linkers (eg: mostly *o*-nitro-benzyl groups), for example, attached to gold nanoparticles as a linker for the direct conjugation of drugs,¹⁸ as part of mesoporous silica nanoparticles¹⁹ and as a crosslinker incorporated in the backbone of polymers.²⁰ The major drawback of those light-triggered drug delivery systems relies on the use of UV irradiation leading to low penetration depth and phototoxicity. During the last twenty years, the challenge in the uncaging field was to overcome the difficulty that only high energy light (*i.e.* damaging biological tissues) can induce photolytic reactions. One strategy to lower phototoxicity by using visible light activation is to tailor the photoremovable protecting groups (PPGs) with extended π -conjugation and introduce heteroatoms and

functional groups in the ring system so that larger dipole change can be generated upon excitation. In particular, blue light-sensitive PPGs have been reported in the coumarin,²¹⁻²⁵ *o*-nitrobenzyl²⁶⁻²⁷ and *o*-nitrophenethyl²⁸ series. To be able to use a red-light activation, the use of upconversion (UC) assisted photolysis has been recently explored to trigger drug delivery upon photolysis from nanocarriers *in vivo*.²⁹⁻³⁰ UC is an anti-Stokes process able to convert photons into higher-energy, allowing for example the conversion of red to blue light. UC systems based on triplet-triplet annihilation upconversion (TTA-UC) of organic chromophores has very recently been applied for life science applications.³¹⁻³⁵ In TTA-UC, photon energies absorbed by (at least) two donor chromophores– also called “sensitizers” – are transferred to emitter chromophores – also called “annihilators” – through collisions resulting in triplet-triplet energy transfer. Then, upon diffusion, two annihilators in their triplet excited state can collide producing one singlet excited state emitting luminescence³⁶⁻³⁸ (see figure S2A).

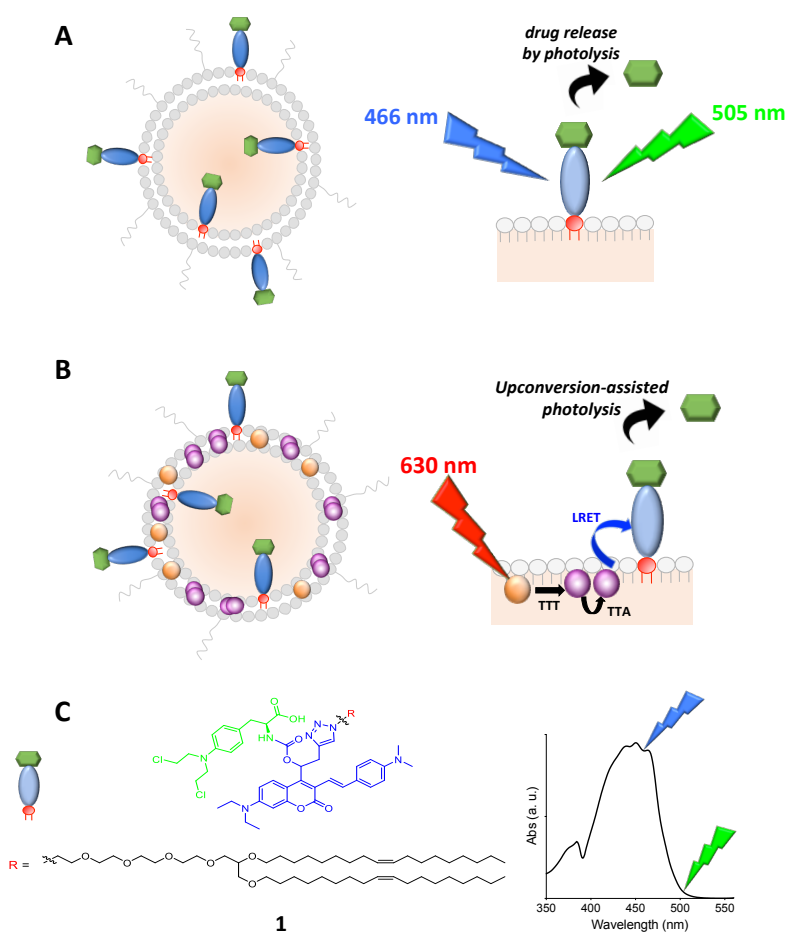


Figure 1: Design of liposomes for light activated surface drug release.

A and B- Design of light-activatable liposome for drug-delivery system using either (A) blue, green or (B) deep-red light irradiation: the caged drug is anchored at the surface of the liposome and can respond directly to blue and green light activation. The upconversion couple can be integrated in the lipid bilayer allowing deep-red light upconversion-assisted photolysis. **C-** Chemical structure of the photoactivatable prodrug **1**, composed of the photocleavable linker (PCL, blue), melphalan (green) and a lipid anchor (R, red) and its absorption spectrum.

Here, we designed liposome-based nanoparticles able to release a payload anchored at the surface of the phospholipid bilayer, using a photolytic reaction. Therefore, a drug conjugated blue light sensitive coumarinyl linker was developed. This latter is based on an efficient blue light sensitive photolabile protecting group modified by a lipid anchor which enables its incorporation into liposomes (Figure 1A). In addition, formulated liposomes were doped with TTA red to blue light upconverting organic chromophores in order to prepare red light sensitive liposomes able to release, by upconversion assisted photolysis, an anticancer drug using a light emitting diode (LED) based photoactivation (Figure 1B). Those light-activatable Lps were used to demonstrate that direct blue or green light photolysis or red light TTA-UC assisted drug-photolysis can effectively photorelease the antitumoral drug melphalan and kill tumor cells *in vitro* after photoactivation.

RESULTS AND DISCUSSION

Design of efficient Lps for light-assisted surface drug release.

To perform a specific drug release at the surface of liposomes by photolysis, a blue light-sensitive photocleavable linker (PL) was prepared. Therefore, a recently developed coumarinyl photoremovable protecting group (PPG), called DEACAS (for structure, see Figure 1A), was selected based on its excellent uncaging efficiency (defined as the product of the uncaging quantum yield [ϕ_u] and the molar extinction coefficient [ϵ] upon blue light-excitation. This photocage already showed an uncaging efficiency $\phi_u \times \epsilon = 8200 \text{ M}^{-1} \text{ cm}^{-1}$ at 446 nm for the release of a carboxylic acid function.²³ This latter compound was modified to bear a lipid anchor which enables its incorporation into lipid-based delivery systems, in particular functionalized liposomes. Thus, a PCL based on the DEACAS PPG was synthesized (see Figure 2), coupled to an anticancer drug (eg: melphalan) and was used for the formulation of 380 to 520 nm sensitive photoactivatable liposomes enabling a light-assisted surface drug release. In order to be able to perform red light induced drug release, we doped our photoactivatable liposomes with TTA-UC chromophores. Therefore, we selected Pd-TPTBP as an organic sensitizer (with an absorption between 615 and 645nm) and *tert*-butylated perylene as an emitter (see Figure S1E). This chromophore pair which has already been encapsulated in liposomes (Lps) enables red to blue light UC. In addition, the use of antioxidants such as sodium sulfite or ascorbic acid have also been reported to prevent oxygen quenching.³⁹ Our system was designed to have an efficient energy transfer, by so-called luminescence resonance energy transfer (LRET) from the *tert*-perylene S1 state resulting from the UC process to the photo-cleavable linker acceptors anchored at the surface of the liposome. Since such transfers depend partly on distance, a short triazole moiety between the PPG and the lipid anchor was introduced to optimize the desired UC-assisted photolysis (see Figure 1B).

The 7- *N,N*-(diethylamino)-2-oxo-2*H*-chromene-4-carbaldehyde **4** was synthesized first in two steps starting from 7-*N,N*-(diethylamino)-4-methyl-2*H*-chromen-2-one **2**.⁴⁰ To introduce a propargyl

function at the benzylic position of the DEACAS PPG, we directly convert the stable aldehyde **4** to the coumarinyl derivative **5**. Using propargyl zincate on aldehyde **4**, analogue **5** was obtained in 86% yield through a Barbier reaction. Compound **5** was converted with 93% yield to the brominated derivative **6** using *N*-bromosuccinimide. We decided then to perform a CuAAC reaction first to graft a dioleoylglycerol (DOG-N₃) lipid anchor⁴¹⁻⁴² to the brominated derivative **6** since the reaction between **6** and freshly prepared *N,N*-dimethyl-4-[(*E*)-2-(4,4,5,5-tetramethyl-1,3,2-dioxaborolan-2-yl)ethenyl]aniline led to the formation of a more rigid coumarinyl PPG through domino reactions initiated by a 5-*exo*-dig cyclocarbopalladation.²⁴ Therefore, **7** was obtained through a copper catalyzed [3+2] cycloaddition with 92% yield. Finally, the DEACAS-DOG **8** was synthesized in 83% yield after a direct Suzuki-Miyaura coupling reaction between **7** and the freshly prepared *N,N*-dimethyl-4-[(*E*)-2-(4,4,5,5-tetramethyl-1,3,2-dioxaborolan-2-yl)ethenyl]aniline.⁴³ Finally, the FDA-approved antitumoral drug for the treatment of multiple myeloma (melphalan) was grafted to **8**. The coupling was performed in two steps using a *p*-nitrophenol carbonate intermediate leading to the formation of DEACAS-DOG-Melph **1** with 82% yield.

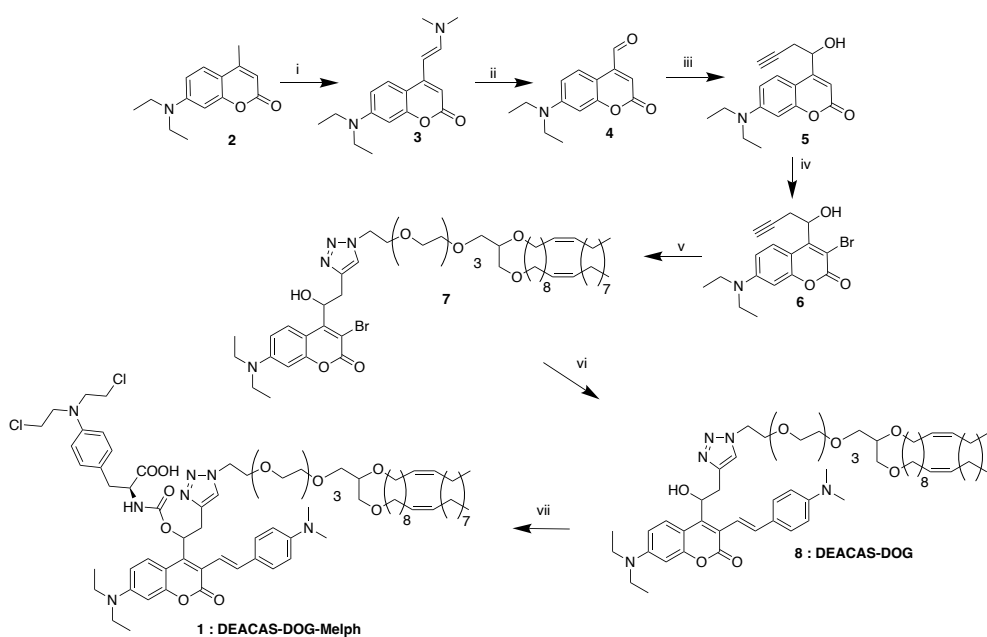


Figure 2: Chemical structures and synthesis of the DEACAS-DOG **8 and DEACAS-DOG-Melph prodrug **1**.**

Synthesis of the fluorescent DEACAS-DOG **8** and the DEACAS-DOG-Melph pro-drug **1**: i) DMF-DMA, DMF, reflux, 16 h, quant., ii) NaIO₄, THF/H₂O, 0 °C to RT, 1 h, 78%, iii) Zinc, propargyl bromide, THF, 0 °C to RT, 1 h 30, 86%, iv) NBS, ammonium acetate, anhydrous acetonitrile, RT, 30 min, 93%, v) (25*Z*)-1-azido-14-[(9*Z*)-octadec-9-en-1-yloxy]-3,6,9,12,16-pentaoxatetradec-25-ene (DOG-N₃), ascorbic acid, distilled CH₂Cl₂, tris(3-hydroxypropyl)triazolmethylamine, tetrakis(acetonitrile)copper (I) hexafluorophosphate, RT, 19 h, 92%, vi) *N,N*-dimethyl-4-[(*E*)-2-(4,4,5,5-tetramethyl-1,3,2-dioxaborolan-2-yl)ethenyl]aniline, K₂CO₃, Pd(PPh₃)₄, H₂O/DME, microwave at 105 °C, 45 min, 83%, vii-a) *p*-nitrophenyl carbonate, DIPEA, DMF, RT, 8 h, vii-b) Melphalan, DMAP, DIPEA, DMF, RT, 4 h 30, 82% over two steps.

Efficient light sensitive Lps for blue, green or red light-assisted surface drug release

The DEACAS-DOG-Melph compound was used in the formulation of Lps with a pro-drug anchored to its surface for a light-assisted drug release. Two liposomal formulations were conceived, the first containing the photo-cleavable prodrug at its surface, called Lp-Prodrug, for direct irradiation with blue and green light. In addition, we prepared previously described Pd-TPTBP and *tert*-butylated perylene doped Lps to develop red light sensitive photoactivatable Lps.³¹ The DEACAS-DOG-Melph compound **1** was again used in this second formulation named Lp-UC-Prodrug with PCLs anchored to its surface for a LRET-assisted drug release (see Figure **1A** and **1B**). Both types of nanoparticles were characterized. Both exhibit a monodispersed and narrow size distribution with a mean diameter of 60 nm for Lp-Prodrug and 97 nm for Lp-UC-Prodrug and both exhibit a slightly negative zeta potential (-7 and -9 mV, respectively), see composition and details in Figure **S1B**.

First, Lp-Prodrug formulation was used to characterize blue-light photolysis. The quantum yields for melphalan release was determined by competition with the DEACAS-*p*-MBA caged analogue as a reference molecule.²³ A quantum yield of 21% for the Lp formulated with 7.8% of DEACAS-DOG-Melph in HEPES 10 mM buffer, pH 7.1 (Figure **3A**) was measured, leading to uncaging efficiencies for 466 nm (blue light) or 505 nm (green light) of $1530 \text{ M}^{-1} \cdot \text{cm}^{-1}$ and $420 \text{ M}^{-1} \cdot \text{cm}^{-1}$ respectively. Noteworthy, those values have been estimated based on the absorption coefficient of the DEACAS chromophore respectively at 466 nm or 505 nm ($\epsilon_{466\text{nm}} = 7300 \text{ M}^{-1} \cdot \text{cm}^{-1}$ and $\epsilon_{505\text{nm}} = 2000 \text{ M}^{-1} \cdot \text{cm}^{-1}$) and on the uncaging quantum yield of **1** formulated in Lps ($\Phi_i = 0.21$).

In addition, we prepared previously described Pd-TPTBP and *tert*-butylated perylene doped Lps, called TTA-UC Lps, to develop red light sensitive Lps.³¹ The DEACAS-DOG compound was again used in the formulation of TTA-UC Lps with PCLs anchored to its surface for a LRET-assisted drug release.

We used fluorescence properties of the DEACAS-DOG **8** to determine the LRET efficiency from the UC system to the DEACAS chromophore in the Lps (see Figures **S3A** and **S3B** for excitation and emission spectra of L-RET donor TBPe and acceptor **8**). Therefore, formulated Lps containing Pd-TPTBP and **8** with TBPe (Lp-UC-**8**) or without TBPe (Lp-Pd-TPTBP-**8**), or with TBPe alone (Lp-UC) were prepared. Upon Pd-TPTBP excitation at 630 nm (which corresponds to the λ_{max} of Pd-TPTBP), the emission profile of Lp-UC-**8** is different from Lp-UC (Figure **3B**), while Lp-Pd-TPTBP-**8** exhibits no fluorescence at all. We quantified the LRET efficiency using absorbance and excitation spectra of the three types of Lps (Figures **S3C** and **S3D**), as described in the method section. The L-RET efficiency was evaluated to be around 50%. This efficient yield results from the specific design of the nanoparticles. The uncaging efficiency at 630 nm (red light) of our photoactivatable nanoplatfrom is therefore estimated around $60 \text{ M}^{-1} \cdot \text{cm}^{-1}$. Noteworthy, this value is based on the absorption coefficient of Pd-TPTBP at 630 nm⁴⁴ ($\epsilon_{630\text{nm}} = 105\,000 \text{ M}^{-1} \cdot \text{cm}^{-1}$), the estimated UC quantum yield ($\Phi_{\text{UC}} = 0.0054$), the

50% LRET efficiency energy transfer of the Lp-UCs to **8**, and the uncaging quantum yield of **1** formulated in Lp ($\Phi_u = 0.21$).

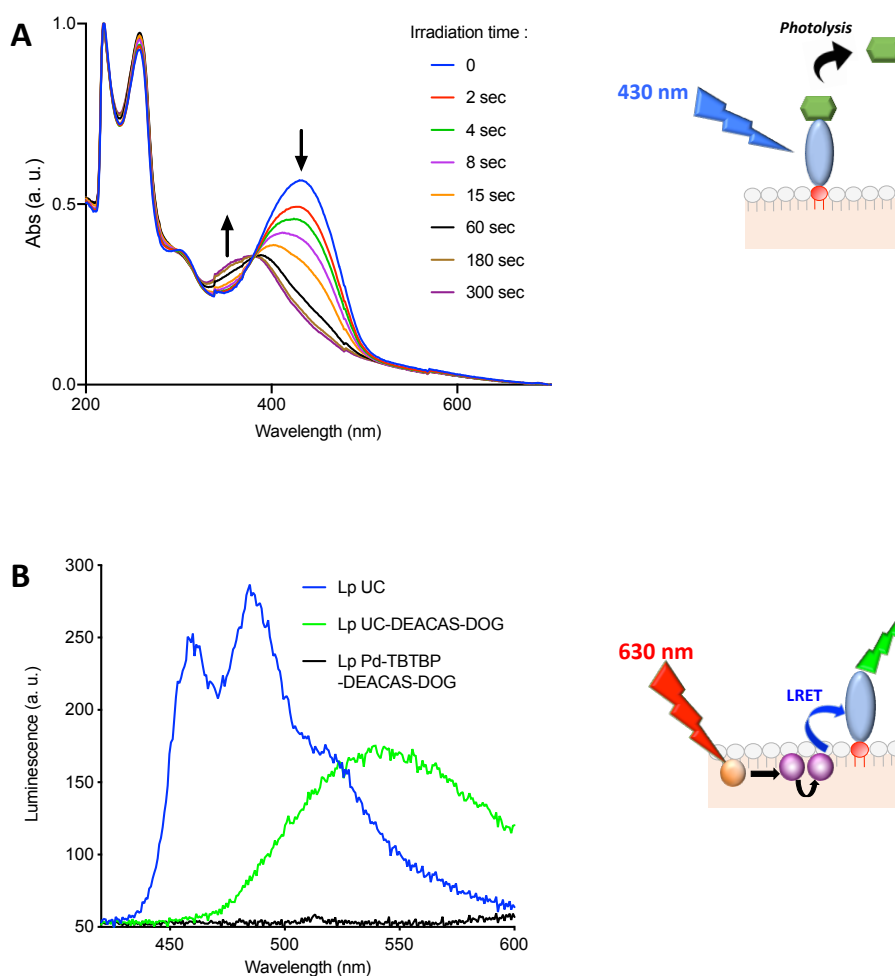


Figure 3: Photochemical characterization of the PCL.

A- UV absorbance after irradiation at 430 nm of 20 μM solutions of Lp-Prodrug. **B-** Emission spectra of Lps (in HEPES buffer supplemented with NaSO_3) upon 630 nm irradiation, UC-doped Lps (Lp-UC, Pd-TPTBP/TBPe, blue), Lps loaded with the UC system and LRET acceptor (Lp-UC-**8**, green), or Pd-TPTBP and LRET acceptor (Lp Pd-TPTBP- **8**, black). $\lambda_{\text{ex}} = 630 \text{ nm}$, $15 \text{ W}\cdot\text{cm}^{-2}$.

Quantification of the blue, green or red light surface drug release and stability of photoactivatable Lps.

The excellent photophysical properties of our Lps bearing a DEACAS PPG at its surface, allowed us to study the ability of the nanoparticles to liberate an anticancer drug (eg. melphalan) after blue to red light excitation. The as-prepared Lps-Prodrug or TTA-UC doped Lps-UC-Prodrug were used to quantify the yield of melphalan release after photolysis, respectively after irradiations at 466 nm, or 505 nm and at 630 nm (using commercial LED light sources, respectively $5 \text{ mW}\cdot\text{cm}^{-2}$, $2 \text{ mW}\cdot\text{cm}^{-2}$ and $5 \text{ mW}\cdot\text{cm}^{-2}$) respectively by HPLC analysis and UV spectroscopy (Figure S5) after membrane filtration (to separate the liposomes from the small molecules). Remarkably, up to 80% of melphalan release from

the external bilayer of our photoactivatable Lps was observed after 10 min, 60 min or 60 min irradiation at respectively 466 nm, 505 nm or 630 nm (Figure 4A-C) indicating, as expected, that our formulation is able to liberate the melphalan very efficiently using a blue light excitation, but that a direct green light excitation can also photorelease the payload. In addition, Lps doped with TTA-UC chromophore were able to release melphalan by UC-assisted photolysis. Importantly, similar results were obtained after 48 hours at 37 °C or after long-term storage at 4 °C (Table 1) indicating that our formulation is stable and still able to induce an efficient payload release after storage. Considering the excellent yields of photoinduced melphalan release reached by our Lps using blue to red light, we next studied the ability of our Lps to kill tumor cells in a light-controlled manner.

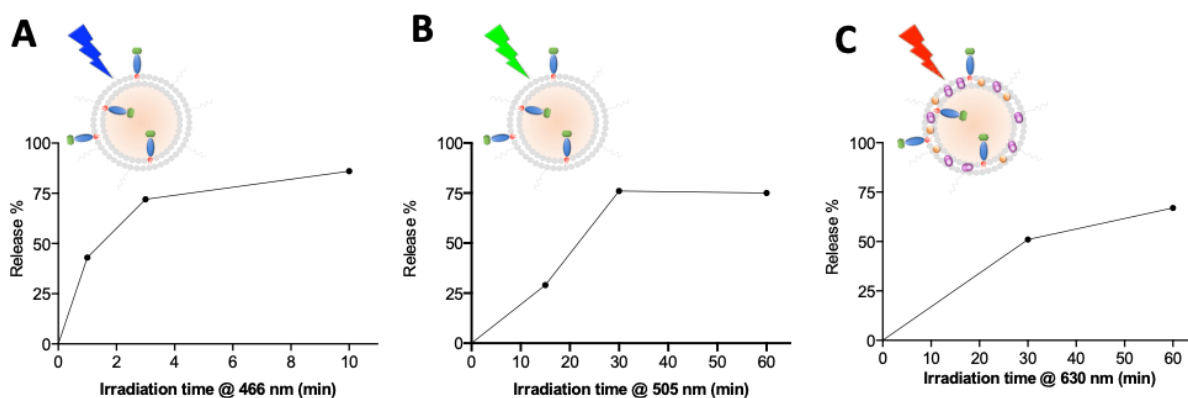


Figure 4: Drug release upon irradiation using different wavelengths.

Quantification of released melphalan from Lp-Prodrug upon 466 nm (A, 5 mW.cm⁻²), 505 nm (B, 2 mW.cm⁻²) or 630 nm (C, 5 mW.cm⁻²) irradiation in HEPES buffer (supplemented with NaSO₃ for 630 nm irradiation), monitored by UV-Visible absorption. Yield of photorelease was extrapolated from quantification of melphalan in buffer.

***In vitro* tumor cell killing using blue, green or red light excitation on photoactivatable Lps**

First, the feasibility of a blue to red light-controlled cell killing was studied. Therefore, we selected a human breast cancer cell line, namely MDA-MB-231 and we evaluated the safety of the different wavelength irradiations. It appeared that 505 nm or 630 nm irradiation for 1 hour and 466 nm irradiation up to 5 min at respectively 2 mW.cm⁻², 5 mW.cm⁻² or 5 mW.cm⁻² were not toxic for the cells (figure S6D and S6E). Furthermore, the treatment of MDA-MB-231 cells with blank or UC-doped liposomes in addition to irradiation at the different wavelengths was not toxic either (figure S7). As previously determined, those irradiation times were in accordance with an almost total release of the drug from the Lps. Thus, the cells were irradiated or not at low light intensity using blue (466 nm, 5 min), green (505 nm, 60 min) or deep-red (630 nm, 60 min) LEDs (see set up characteristics in Figure S6A, S56B and S6C). The results showed that for the 3 different excitation wavelengths with 0.027 mM of phospholipids of Lp-Prodrug or Lp-UC-Prodrug (final

concentration of Pd-TPTBP 0.05 μM , TBPe 0.5 μM , 1.1 μM) a dramatic decrease in the cell viability was observed at each irradiation wavelength (Figure 5A-C).

Light mediated melphalan release		
Storage condition	Irradiation	Drug photorelease
freshly formulated	non irradiated	ND
	430 nm, 10min	86%
4 $^{\circ}\text{C}$ 30 days	non irradiated	ND
	430 nm, 10min	80%
37 $^{\circ}\text{C}$ 48 hours	non irradiated	ND
	430 nm, 10min	79%

Table 1: Formulation of stable light responsive liposomes.

Quantification of released melphalan from Lp-Prodrug stored in different conditions upon 430 nm irradiation (200 mW.cm⁻²), (ND not detected).

Depending on the irradiation wavelengths, the cell viability was reduced by 95 to 82% while in dark condition the viability was similar to untreated cells. Noteworthy, the toxicity of free melphalan (at the same concentration, Figure 5D) was always lower than that of the irradiated prodrug Lps, which can be explained by the enhanced cellular uptake of the prodrug with our Lps and the reported low cellular entry of melphalan.⁴⁵ Also, our results show that our photoactivatable Lps used at 0.027 mM of phospholipids and containing Pd-TPTBP/TBPe are showing similar low toxicity compared to the undoped Lps. We were able to perform a blue light photoactivation using a short irradiation time due to the excellent photosensitivity of our photoactivatable Lps. Moreover, this short irradiation time did not show significant phototoxicity on cells without treatment with photoactivatable Lps (Figure 5D). Therefore, our photoactivatable Lps were able to efficiently release melphalan using blue to red light excitation on cells. In addition, using our irradiation protocols, no significant difference on cell viability was observed among light conditions (with or without blue to red light) indicating that the light sensitivity of our photoactivatable Lps is high enough to selectively induce the photolytic reaction without affecting the cell viability. Therefore, we believe that this type of modified Lps could be applied to the programmed release of several drugs or biological effectors by photoactivation on cells

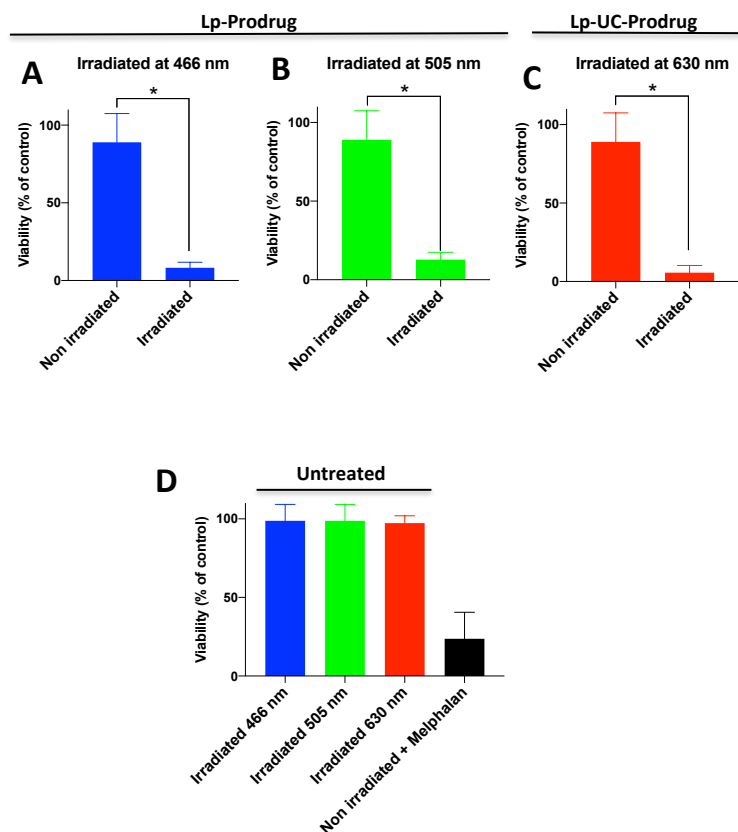


Figure 5: In vitro prodrug activation using blue, green or red light irradiation.

A, B and C - MDA-MB-231 cells were treated with Lp-Prodrug (**A** and **B** = Lp 0.027 mM + 11 μ M) or Lp-UC-Prodrug (**D** = Lp 0.027 mM + Pd-TPTBP 0.05 μ M, TBPe 0.5 μ M, 11 μ M) and then irradiated or not at different wavelengths: 466 nm (**A**, 1.5 J. cm⁻² [5 mW.cm⁻² for 5 min]), 505 nm (**B**, 7.2 J. cm⁻² [2 mW.cm⁻² for 60 min]) or 630 nm (**C**, 18 J. cm⁻² [5mW.cm⁻² for 60 min]), drug to light delay (DLI) 4 hours. Cell viability was monitored at day 8 (n = 3) (* p < 0,01).

D – Untreated MDA-MB-231 cells were irradiated or not at different wavelengths 466 nm (1.5 J. cm⁻² [5 mW.cm⁻² for 5 min]), 505 nm (7.2 J. cm⁻² [2 mW.cm⁻² for 60 min]) or 630 nm (18 J. cm⁻² [5mW.cm⁻² for 60 min]) or non-irradiated but treated with free melphalan (1 μ M). Cell viability was monitored at day 8 (n = 3).

CONCLUSION

In this work, we developed a simple method for the preparation of liposomes able to efficiently release a payload from their surface using blue, green or red light excitation. In particular, we developed an original light-sensitive platform for the preparation of photoactivatable Lps with a precise and covalent surface modification. In addition, we were able to photorelease a payload from the Lps surface using deep red light excitation, due to an efficient (up to 50%) energy transfer from Lps doped by TTA-UC chromophores to the photocleavable protecting group. Furthermore, the DEACAS-DOG lipid **8** was coupled to an antitumoral drug (melphalan) using a stable carbamate linkage, allowing liposome surface modification with a photoactivatable prodrug. Very importantly, the new platform allowed us to release more than 86% of the conjugated melphalan after a blue to red light cell compatible irradiation using LEDs excitations. The Lps showed excellent stability in the dark and they were active *in vitro*, leading to the first report of a stable light-sensitive Lp able to efficiently release a drug in the full visible

spectral region.

In summary, we developed original light-activatable liposomes able to efficiently release an anticancer drug using visible light. Those photoactivatable Lps are not restricted to melphalan release and should allow a great deal of flexibility leading to a wide range of future applications requiring programmed release of drugs or biological effectors by photoactivation.⁶ Therefore, we think that our Lp-based uncaging system offers a new platform for improving the actual performance of photoactivation systems and for future applications in the fields of time resolved biological studies, light targeted drug delivery and photoactivated chemotherapy.

EXPERIMENTAL PROCEDURES

Materials and general procedures

All manipulations of light-sensitive compounds (reactions, purifications, photophysical studies) were performed in the dark with a RGB LED projector MEIKEE (25W) set on the red light (~ 630 nm) and without parasitic light, in particular from computer screens.

The reagents and anhydrous solvents used for the synthesis were ordered to Sigma-Aldrich, TCI EUROPE, Acros Organics or Alfa Aesar. All commercial reagents were used without any further purification except dichloromethane (distilled over CaH₂ under an argon atmosphere) and THF (distilled over sodium/benzophenone under an argon atmosphere) before use.

¹H NMR and ¹³C NMR spectra were recorded at 400 and 101 or 500 and 126 MHz, respectively using the following NMR Bruker instruments: an Avance III 400 MHz spectrometer, an Avance III 500 MHz spectrometer and an Avance II 500 MHz spectrometer equipped with a helium cryoprobe. Chemical shifts (δ) are indicated in ppm with respect to the NMR solvents residual signals (CHCl₃: 7.26 ppm, CH₂Cl₂: 5.32 ppm for ¹H NMR and CDCl₃: 77.16 ppm, CD₂Cl₂: 54.00 ppm for ¹³C NMR). The attributions are given in the following manner: chemical shift followed in parenthesis by i) the multiplicity (s, br, d, t, q, m, dd, dq, dtd and ddd corresponding respectively to singlet, broad, doublet, triplet, quadruplet, multiplet, doublet of a doublet, doublet of a quadruplet, doublet of a triplet of a doublet, doublet of a doublet of a doublet), ii) the number of protons, and iii) the coupling constant in Hz.

The LC-MS mass spectra were carried out using an Agilent LC 1200 series/ QToF 6520 spectrometer. The LC system was run using a ZORBAX RRHD SB-C18 2.1 mm id × 50 mm, 1.8- μ m threaded column and acetonitrile + 0.05% formic acid/mQ H₂O + 0.05% formic acid as elution system. Spectra were acquired by ESI+ ionization (T_{source} = 340 °C, V_{cap} = 4000 V).

Thin Layer Chromatography (TLC) analyses were performed using aluminum plates covered with silica gel 60 F254 Merck. Column chromatography were done on silica gel (230-400 mesh, 0.040-0.063 mm) Merck. Some purifications were performed using thin layer chromatography plates from Miles Scientific (Silica gel GF, UV254, 20x20 cm, 1500 micron).

HPLC analyses were performed on a high-performance chromatography system from Waters® (Waters 1525 pump with Waters 2996 detector) equipped with a Thermo Betabasics 5-micron (4.6, 250 nm) analytical column. Analyses were done using a gradient starting from 100% mQ H₂O acidified with 0.01% of TFA and reaching 100% acetonitrile in 30 min followed by 10 min over 100% acetonitrile. HPLC purifications were performed using a high-performance chromatography Waters system, i.e. Waters 600 double body pump with Waters 2996 detector, equipped with a Thermo Betabasics 5-micron (10 x 250 mm) column. The HPLC purifications were done using a gradient starting from 100% mQ H₂O acidified with 0.01% of TFA and reaching 100% acetonitrile in 30 min.

For the microwave heated reactions, a Monowave 300 from Anton Paar was used with IR temperature monitoring. A heating temperature profile reaching as fast as possible the targeted temperature was used.

meso-Tetraphenyl-tetrabenzoporphine palladium complex (Pd) and tetra-*tert*-butylperylene (TBPe) were obtained from abcr GmbH (Karlsruhe, Germany) and Sigma Aldrich (St. Louis, Missouri, United States) respectively. Sodium chloride (NaCl) was purchased from VWR chemicals (Strasbourg, France) while HEPES was provided from Carl Roth GmbH (Karlsruhe, Germany). Glutathione as well as cell culture media, cell related reagents and MTS [3-(4,5-dimethylthiazol-2-yl)-5-(3-carboxymethoxyphenyl)-2-(4-sulfophenyl)-2*H*-tetrazolium] were purchased from Sigma Aldrich (St. Louis, Missouri, United States) and Promega (Wisconsin, United States) respectively. De-ionised water was obtained from a Milli[®] RO System (Millipore, Paris, France).

Chemical Synthesis

- (*E*)-7-*N,N*-(Diethylamino)-4-(2-(dimethylamino)vinyl)-2*H*-chromen-2-one (**3**)

According to the procedure described in the literature,³⁷ to a solution of 7-*N,N*-(diethylamino)-4-methyl-2*H*-chromen-2-one **2** (5 g, 21.6 mmol, 1 eq.) in anhydrous DMF (50 mL) under Ar, was added DMF-DMA (5.8 mL, 43.2 mmol, 2 eq.). The yellowish solution was heated at reflux under Ar during 19 h. A saturated aqueous solution of NaHCO₃ was then added and the aqueous phase was extracted 3 times with CH₂Cl₂. The combined organic layers were dried over Na₂SO₄, filtered and concentrated under vacuum to afford the titled product **3** as an amorphous yellow solid (6.19 g, quant.).

R_f = 0.30 (CH₂Cl₂/EtOAc 7:3 in vol.); ¹H NMR (400 MHz, CDCl₃): δ 7.52 (d, *J* = 9.0 Hz, 1H), 7.21 (d, *J* = 13.0 Hz, 1H), 6.54 (dd, *J* = 9.0, 2.7 Hz, 1H), 6.49 (d, *J* = 2.7 Hz, 1H), 5.85 (s, 1H), 5.22 (d, *J* = 13.0 Hz, 1H), 3.39 (q, *J* = 7.1 Hz, 4H), 2.99 (s, 6H), 1.19 (t, *J* = 7.1 Hz, 6H).

- 7- *N,N*-(Diethylamino)-2-oxo-2*H*-chromene-4-carbaldehyde (**4**)

50 mL of a mixture of THF/H₂O (1:1 in vol.) were added to the previously formed enamine **3** (6.19 g, 21.6 mmol, 1 eq.). NaIO₄ (13.87 g, 64.9 mmol, 3 eq.) was added slowly at 0 °C and a brownish suspension was obtained. It was stirred at 0 °C during 10 min and then the cold bath was removed. Few minutes later, a dark precipitate was obtained. The precipitate was filtered over a pad of celite after 1 h and rinsed with CH₂Cl₂. The solvent was evaporated under vacuum and the residue was taken up with CH₂Cl₂. A saturated aqueous solution of NaHCO₃ was added to the dark reddish solution and the organic phase was separated. The aqueous phase was extracted four times with CH₂Cl₂. The combined organic phases were dried over MgSO₄, filtered and concentrated under vacuum. The dark reddish oil was rapidly filtered on a thin pad of silica with CH₂Cl₂ to afford the titled compound **4** as a dark reddish solid (4.11 g, 78%).

R_f = 0.45 (CH₂Cl₂); ¹H NMR (400 MHz, CDCl₃): δ 10.03 (s, 1H), 8.31 (d, *J* = 9.2 Hz, 1H), 6.63 (dd, *J* = 9.2, 2.7 Hz, 1H), 6.52 (d, *J* = 2.7 Hz, 1H), 6.46 (s, 1H), 3.43 (q, *J* = 7.1 Hz, 4H), 1.22 (t, *J* = 7.1 Hz, 6H).

- 7- *N,N*-(Diethylamino)-4-(1-hydroxybut-3-yn-1-yl)-2*H*-chromen-2-one (**5**)

Zn dust (2 g) was activated 1 min with diluted HCl (2M), washed (1 min) with H₂O (3x), EtOH (2x) and anhydrous diethyl ether (x2) and finally dried under reduced pressure.

This activated zinc (1.79 g, 27.3 mmol, 6.4 eq.) was suspended under Ar in dry THF (14.3 mL) and propargyl bromide (80 wt. % solution in toluene) (1.27 mL, 11.4 mmol, 2.7 eq.) was added dropwise at 0 °C. The reaction mixture was stirred at 0 °C for 1 h 30. Then a suspension of the freshly prepared propargylzinc bromide in THF (14.5 mL, 2.5 eq.) was added to aldehyde **4** (1.05 g, 4.27 mmol, 1 eq.). After completion of the reaction (1 h 30), the mixture was quenched by adding a saturated aqueous solution of NH₄Cl and extracted with CH₂Cl₂. The combined organic layers were dried over Na₂SO₄, filtered and evaporated under reduced pressure. The residue was purified by column chromatography (0 to 40% heptane/EtOAc in vol.) to afford the title compound **5** as an amorphous yellow solid (1.05 g, 86%).

R_f = 0.52 (CH₂Cl₂/EtOAc 8:2 in vol.); ¹H NMR (400 MHz, CDCl₃): δ 7.39 (d, *J* = 9.0 Hz, 1H), 6.57 (dd, *J* = 9.0, 2.6 Hz, 1H), 6.51 (d, *J* = 2.6 Hz, 1H), 6.29 (d, *J* = 1.0 Hz, 1H), 5.13 (dtd, *J* = 7.7, 4.2, 1.0 Hz, 1H), 3.40 (q, *J* = 7.1 Hz, 4H), 2.83 (ddd, *J* = 17.0, 4.2, 2.6 Hz, 1H), 2.68 (d, *J* = 4.2 Hz, 1H), 2.63 (ddd, *J* = 17.0, 7.7, 2.6 Hz, 1H), 2.17 (t, *J* = 2.6 Hz, 1H), 1.20 (t, *J* = 7.1 Hz, 6H).

- 3-Bromo-7-(diethylamino)-4-(1-hydroxybut-3-yn-1-yl)-2H-chromen-2-one (6)

7-(Diethylamino)-4-(1-hydroxybut-3-yn-1-yl)-2H-chromen-2-one **5** (250 mg, 0.88 mmol, 1 eq.) was dissolved in distilled acetonitrile (4.2 mL). NBS (171.5 mg, 0.96 mmol, 1.1 eq.) and ammonium acetate (6.8 mg, 0.1 mmol, 0.1 eq.) were added under Ar. After 30 min stirring, the mixture was poured into water and extracted with EtOAc. The combined organic layers were dried over Na₂SO₄, filtered and evaporated under vacuum. The product was purified by column chromatography (25% EtOAc/heptane in vol.) to afford the title compound **6** as an amorphous yellow solid (297 mg, 93%).

R_f = 0.82 (EtOAc/CH₂Cl₂/ 2:8 in vol.); ¹H NMR (400 MHz, CDCl₃): δ 8.22 (d, *J* = 9.4 Hz, 1H), 6.57 (dd, *J* = 9.4, 2.7 Hz, 1H), 6.45 (d, *J* = 2.7 Hz, 1H), 5.60 (dd, *J* = 9.2, 5.1 Hz, 1H), 3.40 (q, *J* = 7.1 Hz, 4H), 2.91 (ddd, *J* = 16.8, 9.2, 2.6 Hz, 1H), 2.75 (ddd, *J* = 16.8, 5.1, 2.6 Hz, 1H), 2.13 (t, *J* = 2.6 Hz, 1H), 1.20 (t, *J* = 7.1 Hz, 6H); ¹³C NMR (101 MHz, CDCl₃): δ 158.3, 155.4, 152.8, 150.6, 127.8, 108.9, 106.4, 104.3, 97.5, 79.6, 73.8, 71.7, 44.9, 26.1, 12.6; HR-MS (ESI, positive mode): *m/z* [M+H]⁺ calculated for C₁₇H₁₉BrNO₃: 364.0543, found: 364.0530.

- 3-Bromo-7- *N,N*-(diethylamino)-4-(1-hydroxy-2-(1-((*Z*)-14-(((*Z*)-octadec-9-en-1-yl)oxy)-3,6,9,12,16-pentaoxatetatriacont-25-en-1-yl)-1H-1,2,3-triazol-4-yl)ethyl)-2H-chromen-2-one (7)

(*Z*)-1-Azido-14-(((*Z*)-octadec-9-en-1-yl)oxy)-3,6,9,12,16-pentaoxatetatriacont-25-ene (114 mg, 0.14 mmol, 1 eq.), previously prepared as described in the literature,³⁸⁻³⁹ was diluted under argon in distilled CH₂Cl₂ (1.7 mL) and 3-bromo-7-*N,N*-(diethylamino)-4-(1-hydroxybut-3-yn-1-yl)-2H-chromen-2-one **6** (62.7 mg, 0.17 mmol, 1.2 eq.), ascorbic acid (75.8 mg, 0.43 mmol, 3 eq.) and tris(3-hydroxypropyl)triazolylmethylamine (56.1 mg, 0.13 mmol, 0.9 eq.) were added to the solution. Three “freeze-pump-thaw” cycles were performed before adding Cu(CH₃CN)₄PF₆ (53.5 mg, 0.14 mmol, 1 eq.) and one of these cycles was done again. The mixture was stirred at room temperature during 19 h. Then the media was poured into water and extracted with EtOAc. The combined organic layers were washed with brine, dried over Na₂SO₄, filtered and concentrated under vacuum. The product was purified by preparative TLC with 5% MeOH/CH₂Cl₂ in vol. as eluent to afford the title compound **7** as a yellow solid (152.8 mg, 92%).

R_f = 0.36 (CH₂Cl₂/MeOH 95:5 in vol.); ¹H NMR (400 MHz, CDCl₃): δ 8.44 (d, *J* = 9.3 Hz, 1H), 7.73 (s, 1H), 6.58 (dd, *J* = 9.3, 2.7 Hz, 1H), 6.49 (d, *J* = 2.7 Hz, 1H), 5.69 (dt, *J* = 10.2, 3.3 Hz, 1H), 5.47–5.25 (m, 4H), 4.55 (t, *J* = 4.9 Hz, 2H), 4.46 (s, 1H), 3.87 (t, *J* = 4.9 Hz, 2H), 3.66–3.56 (m, 12H), 3.53–3.35 (m, 14H), 3.14 (dd, *J* = 15.2, 3.3 Hz, 1H), 2.03–1.96 (m, 8H), 1.56–1.46 (m, 4H), 1.36–1.23 (m, 44H), 1.20 (t, *J* = 7.1 Hz, 6H), 0.87 (t, *J* = 6.8 Hz, 6H); ¹³C NMR (126 MHz, CDCl₃): δ 158.3, 155.5, 154.2, 150.5, 130.4, 130.1, 130.0, 128.5, 123.5, 108.8, 106.9, 103.8, 97.5, 78.0, 75.1, 71.8, 71.5, 71.0, 70.8 (3 signals), 70.7 (3 signals), 70.6, 69.6, 50.5, 44.9, 32.7, 32.0, 31.9, 30.2, 29.9 (2 signals), 29.8 (2 signals),

29.7 (3 signals), 29.6, 29.5 (2 signals), 29.3, 27.4, 26.3, 26.2, 22.8, 21.2, 14.3, 12.6 ; HR-MS (ESI, positive mode): m/z $[M+Na]^+$ calculated for $C_{64}H_{109}BrN_4O_9Na$: 1179.7270, found: 1179.7312.

- 7- *N,N*-(Diethylamino)-3-((*E*)-4- *N,N*-(dimethylamino)styryl)-4-(1-hydroxy-2-(1-((*Z*)-14-(((*Z*)-octadec-9- en-1-yl)oxy)-3,6,9,12,16-pentaoxatetracont-25-en-1-yl)-1*H*-1,2,3-triazol-4-yl)ethyl)-2*H*- chromen-2-one (DEACSAS-DOG **8**)

Under Ar, a microwaved tube was filled with *N,N*-dimethyl-4-[(*E*)-2-(4,4,5,5-tetramethyl-1,3,2-dioxaborolan-2-yl)ethenyl]aniline (71.73 mg, 0.26 mmol, 1.3 eq.) previously prepared according to the literature,⁴⁰ K_2CO_3 (27.9 mg, 0.2 mmol, 1 eq.), and a solution of the substrate **7** (234 mg, 0.2 mmol, 1 eq.) in DME (3 mL). Distilled water (1 mL) was added to this mixture. Three “freeze-pump-thaw” cycles were performed before adding $Pd(PPh_3)_4$ (4.7 mg, 4 μ mol, 0.02 eq.) and one of these cycles was done again after the addition. The sealed tube was allowed to warm up to room temperature and was microwaved at 105 °C during 50 min. The solution turned orange. The TLC showed remaining starting material. Hence the tube was frozen and more $Pd(PPh_3)_4$ (4.7 mg, 4 μ mol, 0.02 eq.) and *N,N*-dimethyl-4-[(*E*)-2-(4,4,5,5-tetramethyl-1,3,2-dioxaborolan-2-yl)ethenyl]aniline (27.6 mg, 0.1 mmol, 0.5 eq.) were added under Ar. One “freeze-pump-thaw” cycle was done to remove oxygen and then the sealed tube was allowed to warm up to room temperature under Ar. The sealed tube was microwaved at 105 °C during 30 min. The mixture was then poured into a saturated aqueous solution of $NaHCO_3$ and was extracted with EtOAc. The combined organic layers were dried over $MgSO_4$, filtered and concentrated under vacuum. The product was purified with preparative TLC with EtOAc/heptane 8:2 in vol. as eluent, to afford the title compound **8** as a yellow solid (205 mg, 83%).

R_f = 0.79 (CH_2Cl_2 /EtOAc 8:2 in vol.); 1H NMR (400 MHz, $CDCl_3$): δ 8.24 (d, J = 9.2 Hz, 1H), 7.65 (s, 1H), 7.40–7.31 (m, 3H), 6.99 (d, J = 16.2 Hz, 1H), 6.66 (d, J = 8.8 Hz, 2H), 6.57 (dd, J = 9.2, 2.7 Hz, 1H), 6.50 (d, J = 2.7 Hz, 1H), 5.75 (dd, J = 9.8, 3.7 Hz, 1H), 5.45–5.27 (m, 4H), 4.50 (dd, J = 5.7, 4.3 Hz, 2H), 3.99 (s, 1H), 3.84–3.79 (m, 2H), 3.61–3.53 (m, 13H), 3.52–3.35 (m, 13H), 3.19 (dd, J = 15.4, 3.7 Hz, 1H), 2.96 (s, 6H), 2.03–1.90 (m, 8H), 1.56–1.46 (m, 4H), 1.35–1.23 (m, 44H), 1.21 (t, J = 7.1 Hz, 6H), 0.87 (t, J = 6.8 Hz, 6H) ; ^{13}C NMR (101 MHz, $CDCl_3$): δ 161.7, 155.1, 150.4, 149.6, 148.6, 144.7, 135.3, 132.2, 130.5, 130.4, 130.1, 130.0, 128.3, 128.0, 126.4, 123.5, 116.7, 116.5, 112.5, 108.6, 107.6, 97.7, 78.0, 71.8, 71.5, 70.9, 70.8, 70.7 (2 signals), 70.6 (2 signals), 70.5, 69.7, 50.4, 44.8, 40.6, 32.9, 32.8, 32.0, 30.2, 29.9 (2 signals), 29.8 (2 signals), 29.7 (3 signals), 29.6, 29.5 (2 signals), 29.4, 29.3, 27.4, 26.3, 26.2, 22.8, 14.3, 12.7 ; HR-MS (ESI, positive mode): m/z $[M+Na]^+$ calculated for $C_{74}H_{121}N_5O_9Na$: 1246.9057, found: 1246.9105.

- (2*S*)-3-(4-(Bis(2-chloroethyl)amino)phenyl)-2-(((1-(7-*N,N*-(diethylamino)-3-((*E*)-4-*N,N*-(dimethylamino)styryl)-2-oxo-2*H*-chromen-4-yl)-2-(1-((*Z*)-14-(((*Z*)-octadec-9-en-1-yl)oxy)-3,6,9,12,16-pentaoxatetracont-25-en-1-yl)-1*H*-1,2,3-triazol-4-yl)ethoxy)carbonyl)amino)propanoic acid (DEACAS-DOG-Melph **1**)

To 7-*N,N*-(diethylamino)-3-((*E*)-4-(dimethylamino)styryl)-4-(1-hydroxy-2-(1-((*Z*)-14-(((*Z*)-octadec-9-en-1-yl)oxy)-3,6,9,12,16-pentaoxatetracont-25-en-1-yl)-1*H*-1,2,3-triazol-4-yl)ethyl)-2*H*-chromen-2-one **8** (33 mg, 0.027 mmol, 1 eq.) were successively added under Ar and in the dark, 1 mL of anhydrous DMF, DIPEA (9 μ L, 0.05 mmol, 2 eq.) and *para*-nitrophenyl carbonate (12.3 mg, 0.04 mmol, 1.5 eq.). After stirring the resulting mixture at room temperature during 8 h, the volatiles were removed by rotary evaporation. The next reaction was then launched without purification. R_f (*p*-nitrophenylcarbonate intermediate) = 0.75 (CH₂Cl₂/EtOAc 8:2 in vol.). To the so-formed 7-(diethylamino)-3-((*E*)-4-(dimethylamino)styryl)-4-(1-hydroxy-2-(1-((*Z*)-14-(((*Z*)-octadec-9-en-1-yl)oxy)-3,6,9,12,16-pentaoxatetracont-25-en-1-yl)-1*H*-1,2,3-triazol-4-yl)ethyl)-2*H*-chromen-2-one-*para*-nitrophenyl carbonate intermediate were successively added under Ar and in the dark, melphalan (10.6 mg, 0.035 mmol, 1.3 eq.), 1 mL of anhydrous DMF, DIPEA (12 μ L, 0.07 mmol, 2.6 eq.) and DMAP (3.3 mg, 0.027 mmol, 1 eq.). After 4 h 30 stirring at room temperature, the media was concentrated under reduced pressure and the product was purified by preparative TLC with 5% in vol. of MeOH/CH₂Cl₂. The title product **1** was obtained as a mixture of 2 diastereomers as a reddish solid (34 mg, 82% over two steps). R_f = 0.38 (CH₂Cl₂/MeOH 99.5/0.5 in vol.); ¹H NMR (500 MHz, CD₂Cl₂): δ 7.72–7.42 (m, 2H, CH_{triazol} + CH_{5coumarin}), 7.42–7.29 (m, 2H, CH_{aniline part}), 7.40–7.20 (m, 1H, CH_{alkene styryl moiety}), 7.08–7.00 (m, 1H, CH_{aromatic melphalan}), 7.00–6.80 (m, 1H, CH_{alkene styryl moiety}), 6.92–6.83 (m, 1H, CH_{aromatic melphalan}), 6.75–6.65 (m, 2H, CH_{aniline part}), 6.64–6.56 (m, 1H, CH_{aromatic melphalan}), 6.64–6.41 (m, 1H, CH_{6coumarin}, 2 diastereomers), 6.56–6.32 (m, 1H, CH_{8coumarin}, 2 diastereomers), 6.50–6.45 (m, 1H, CH_{benzylic coumarin}), 6.49–6.31 (m, 1H, CH_{aromatic melphalan}), 5.40–5.33 (m, 4H, CH_{alkene fatty chain}), 4.53–4.44 (m, 1H, CH_{melphalan}), 4.43–4.29 (m, 2H, CH_{2melphalan}), 3.69–3.56 and 3.38–3.21 (m, 2H, CH_{2coumarin}), 3.56–3.46 (m, 1H, CH_{glycol}), 3.73–3.38 (m, 32H, CH_{2O}, CH_{2Nmelphalan}, CH_{2melphalan} and CH_{2Clmelphalan}), 3.46–3.39 (m, 4H, CH_{2Ncoumarin}), 2.97 and 2.96 (2s, 6H, CH_{3Ncoumarin}, 2 diastereomers), 2.07–1.93 (m, 8H, CH_{2CHalkene fatty chain}), 1.55–1.48 (m, 4H, CH_{2fatty chain}), 1.35–1.25 (m, 44H, CH_{2fatty chain}), 1.22 and 1.14 (2t, 6H, *J* = 7.1 Hz, CH_{2CH3coumarin}, 2 diastereomers), 0.88 (t, 6H, *J* = 6.90 Hz, CH_{3fatty chain}) ; ¹³C NMR (126 MHz, CD₂Cl₂): δ 174.6, 163.1, 161.4, 158.7 and 158.5 (for 2 diastereomers), 155.3, 155.2, 151.0, 150.2 and 150.1 (for 2 diastereomers), 145.6 and 145.5 (for 2 diastereomers), 143.3 and 143.1 (for 2 diastereomers), 135.6, 135.2, 132.6 and 132.5 (for 2 diastereomers), 131.3, 131.1 and 130.9 (for 2 diastereomers), 130.9 (2 signals for 2 diastereomers), 130.4 (2 signals), 129.2 and 129.1 (for 2 diastereomers), 128.4 and 128.3 (for 2 diastereomers), 124.0, 112.9, 112.4 (2 signals), 109.3, 97.9 and 97.8 (for 2 diastereomers), 78.5 and 78.3 (for 2 diastereomers), 73.1 and 72.3 (for 2 diastereomers), 72.1

(2 signals), 71.8, 71.7, 71.3, 71.2, 71.0 (2 signals), 70.9 (2 signals), 70.0 and 69.9 (for 2 diastereomers), 56.5, 53.8 (under the signal of CD₂Cl₂), 51.0, 50.8, 45.2, 41.3, 41.2 and 41.1 (for 2 diastereomers), 40.8, 33.2, 32.5 (2 signals), 30.7, massif with [30.4 (2 signals), 30.3 (2 signals), 30.1 (2 signals), 29.9 (2 signals) 29.8, 29.7], 27.7, massif with [26.7 (3 signals)], 23.3, 14.5, 13.0 ; HR-MS (ESI, positive mode): m/z [M+Na]⁺ calculated for C₈₈H₁₃₇Cl₂N₇O₁₂Na: 1576.9594, found: 1576.9605.

Liposome (Lp) formulation

Lp were prepared by the lipid film hydration technique. Therefore, lipids and our synthesized compounds (**8** or **1**) (see Figure S1A for composition) were mixed in a round-bottom Pyrex[®] tube in solution in chloroform/methanol (9/1 v/v) and dried under high vacuum for 45 min. To form multilamellar vesicles (MLV), the lipid film was rehydrated in 10 mM HEPES, 150 mM NaCl, pH 7.1 at a final phospholipid concentration of 10 mM. For the formulation of Lp-UC-Prodrug anti-oxydants were added to the buffer: either 10 mM ascorbic acid (for cell culture experiments) or Na₂SO₃ (for spectroscopic measurements). The MLV suspension was sonicated during 1 h at room temperature under a continuous flow of argon using a Vibra Cell 75041 ultrasonicator (750 W, 20 kHz, Fisher Bioblock Scientific, Waltham, United States) equipped with a 3 mm-diameter tip probe (40% amplitude) (1 s cycle every 3 s). At the end of the formulation process, the small unilamellar vesicle (SUV) preparation was centrifuged at 13000 g for 15 min to remove the titanium dust coming from sonication probes.

Particle size measurements

The average diameter of liposomes were determined by dynamic light scattering using a Zetasizer Nano-ZS (MalvernPanalytical, UK) and the following specifications: temperature: 25 °C; viscosity: 1.014 cP; scattering angle: 90°; refractive index: 1.34. Lp were diluted at 1/100 in 10 mM HEPES buffer, 150 mM NaCl, pH 7.1 for three consecutive measurements. Data were analyzed using the multimodal number distribution software of the Zetasizer constructor. Particle size is expressed in intensity. The formulation was considered as monodisperse if the polydispersity index (PDI) is < 0.3.

Particle Zeta-potential measurements

Lp were diluted at 1/50 in water to determine Zeta-potential on a Zetasizer Nano-ZS as previously reported by Brion *et al.* in 2023.³⁵

Determination of the photochemical quantum yield

The uncaging quantum yield was determined in MeOH/H₂O 9:1 in vol. for the DEACAS-DOG-Melph and in HEPES 10 mM, NaCl 150 mM, pH 7.2 for Liposomes formulated with the DEACAS-DOG-Melph, at 25 °C by comparison with the DEACAS-*p*-methoxybenzoic acid as previously reported by Brion *et al.* in 2023.³⁵

Quantification of melphalan release from the surface of the liposomes

Lp containing the DEACAS-DOG-Melph were formulated as previously described, and diluted in 10 mM HEPES buffer, 150 mM NaCl, pH 7.1 prior to irradiation. Samples were irradiated using either 430 nm (using a LUMOS 43 LED source from Atlas Photonics Inc. based on UV-LED technology, with a typical output of 200 mW.cm^{-2} and the wavelength of irradiation was set to 430 nm), 466 nm (5 mW.cm^{-2}), 505 nm (2 mW.cm^{-2}) or 641 nm (5 mW.cm^{-2}) LEDs light source (see below). Then, to investigate the direct drug release, we performed membrane filtration of the samples using ultrafiltration unit (vivaspin 20) equipped with a 100 kDa cut-off semipermeable membrane (Sartorius Stedim Biotech, Aubagne, France), allowing the separation of the irradiated nanoparticles from the released drug. Vivaspin unit was then centrifuged at 5000 g for 20 min. To evaluate the concentration of photoreleased melphalan, the eluate was analyzed either by UV-Visible absorbance or HPLC. As only half of the drug that can be released is available at the outer surface of the liposome (the other half is trapped in the core of the particle) the released percentage of melphalan is expressed in regard of the amount available for measurement in the buffer after photolysis (this means that if 50% of the total amount of melphalan contained in the Lps are released, it corresponds to 100% of uncaging of the melphalan that is on the outer face of the nanoparticles).

Determination of the LRET efficiency

We carried out UV-Vis spectroscopic measurements in a 3 mm spectroscopic cuvette on a Safas Xenius XC apparatus. The same apparatus was used for fluorescence spectra recordings (except for 630 nm irradiation experiments). The fluorescence experiments were performed using Lp formulations diluted 1/100 in 10 mM HEPES buffer, 150 mM NaCl, pH 7.1 containing either 10 mM ascorbic acid or 50 mM Na_2SO_3 .

To measure the TBPe to **8** LRET efficiency E_{LRET} , we proceeded as in Brion *et al.* 2023³⁵ and evaluated E_{LRET} from the excitation spectra of two types of Lps (See Figures **S3C** and **S3D**) loaded with the UC chromophore pair (Pd-TPTBP 20 μM , TBPe 200 μM) and with (a: Lp-UC-**8**) or without (c: Lp-UC) the LRET acceptor (**8**, 280 μM). A third type (b: Lp-Pd-TPTBP-**8**) missing the TBPe (Pd-TPTBP 20 μM , **8** 280 μM) was used to evaluate luminescence signal upon direct **8** excitation.

In Figure **S3C**, we define A_A and A_D as the absorbance at 414 nm of the Acceptor (compound **8** in this experiment) (sample b) and of the Donor TBPe (sample c), respectively, in the Lp. Since Pd-TPTBP does also absorb around 440 nm (not shown) but not at 414 nm, we chose 414 nm as the reference wavelength for the LRET efficiency evaluation. Figure **S3D**, F_A^A and F_A^D represent the Acceptor (**8**) fluorescence signals detected upon 414 nm excitation of this latter compound (sample b), or of the Donor (evaluated from the linear combination of the three samples emissions: (a)-(b)-(c), respectively).

Consequently, LRET efficiency E_{LRET} is given by:

$$E_{LRET} = \frac{F_A^D / (1 - 10^{-A_D})}{F_A^A / (1 - 10^{-A_A})}$$

Evaluating A_D , A_A , F_A^A , F_A^D at 414 nm as illustrated by the arrows in Figures S3C and S3D, we determined $E_{LRET} = 51\%$ (where we evaluate the uncertainty to $\pm 5\%$).

LED irradiation sources for the *in vitro* experiments

For 630 nm irradiation we conceived a homemade apparatus which consists of 4 raw connected in parallel of 9 LEDs (red LED, 636 nm, 1100 mCd, Mouser 696-SSL-LX509E3SIT) connected in series. LEDs were soldered by group of 3 to irradiate all wells of a 12-wells plate. We also designed a 3D printed case to support 12-well plates. A variable laboratory power supply (BaseTech BT-305) was used to power the LED array with controlled voltage and intensity. For each well the light power was measured using a Thorlabs PM100D power meter.

For 466 nm and 505 nm irradiation, homemade irradiation apparatus were also conceived in a similar manner for our studies on 96-well plates.

Spectra of LEDs used in this apparatus are shown in Figure S6A, S6B and S6C using our irradiation conditions ($\lambda_{\max} = 467$ nm, 508 nm and 628 nm respectively, acquired using a Thunder Optics SMA-E spectrometer).

Cell culture, *in vitro* irradiation, and cytotoxicity

Human breast cancer cell line, MDA-MB-231 was obtained from ATCC. Cells were cultured in RPMI-1640 growth medium (Sigma Aldrich, UK), with penicillin and streptomycin (100 IU/mL /100 mg/mL) and 10% FBS (Fetal Bovine Serum). The cells were kept at 37 °C in a cell incubator at 95% relative humidity with 5% CO₂.

For NIR irradiation, MDA-MB-231 cells were plated at 1.6×10^4 cells per mL in 12-well plates. 24 hours after seeding, the cells were treated with Lp. The final concentration in each well was 27 μ M of phospholipids of Lp, 1 μ M of DEACAS-DOG-Melph, 0.5 μ M of TBPe and 0.05 μ M of Pd-TPTBP. Then, a drug to light delay (DLI) of 4 hours was observed, before irradiation at 641 nm (5 mW.cm⁻²). After 7 days, cell viability was evaluated by trypan blue staining using Countess 2 FL automated cell counter (ThermoFischer, Waltham, United States).

For blue and green light irradiation, cells were plated in 96-well plates at 15×10^3 cells per well of complete medium. 24 hours after seeding, the cells were treated with Lp. The final concentration in each well was 27 μ M of phospholipids of Lp, leading to a final concentration of 1 μ M of DEACAS-DOG-Melph. Then, a DLI of 4 hours was observed, before irradiation at 466 nm (5 mW.cm⁻²) or 505 nm (2 mW.cm⁻²). Cell viability was evaluated after 2 or 3 days, using MTS assay (CellTiter 96®

AQ_{ueous} One Solution Cell Proliferation Assay). Briefly, 20 μ L of MTS were added to each well and after 30 min at 37°C the absorbance was measured at 490 nm using a microplate reader (Safas SP2000, Xenius 5801).

All *in vitro* experiments were conducted in technical and biological triplicates.

Statistical analysis

All *in vitro* and biochemical experiments were conducted in triplicate and data are presented as mean \pm SEM. One-way (ANOVA) were performed to address the significance of the differences between the different conditions. Significant difference was concluded when $p < 0.05$.

ASSOCIATED CONTENT

Supporting Information

NMR spectra for all compounds and Figures S1–S7

AUTHOR INFORMATION

Author contributions

J.C. M.K. and A.S. synthesized photoremovable linkers, J.C S.C. and A.S. characterized the chemicals, J.C. A.B. J.L. F.B. and A.S. performed the photophysical and photochemical characterizations, A.B. L.O. B.H. F.B. B.F. and A.K. performed the *in vitro* experiments. All the authors analyzed the data, A.B. A.K. and A.S. wrote the paper. All authors discussed the results and commented on the manuscript, A.S., B.H. and A.K. designed the study and supervised the project.

ACKNOWLEDGEMENTS

This work was supported by the Université de Strasbourg, the CNRS, and by a Grant from the Agence Nationale de la Recherche (Contract No. ANR-18-CE09-0016). JL acknowledges the Interdisciplinary Thematic Institute QMat as part of the ITI 2021-2028 program of the University of Strasbourg, CNRS and Inserm via the IdEx Unistra (ANR 10 IDEX 0002), SFRI STRAT'US (ANR 20 SFRI 0012), and Labex NIE (ANR-11-LABX-0058-NIE) projects of the French Investments for the Future Program. BF and BH acknowledge the Interdisciplinary Institute HiFunMat, as part of the ITI 2021-2028 program of the University of Strasbourg, CNRS and Inserm via the IdEx Unistra (ANR-10-

IDEX-0002) and SFRI-STRAT'US (ANR-20-SFRI-0012) under the framework of the French Investments for the Future Program. AK acknowledges the Interdisciplinary Institute InnoVec, as part of the ITI 2021-2028 program of the University of Strasbourg, CNRS and Inserm, via the IdEx Unistra (ANR-10-IDEX-0002) and SFRI-STRAT'US (ANR-20-SFRI-0012) under the framework of the French Investments for the Future Program.

Conflict of interest

The authors declare no conflict of interest.

REFERENCES

- (1) Allen, T. M.; Cullis, P. R. Liposomal drug delivery systems: from concept to clinical applications. *Advanced drug delivery reviews* **2013**, *65* (1), 36-48. DOI: 10.1016/j.addr.2012.09.037.
- (2) Sainaga Jyothi, V. G. S.; Bulusu, R.; Venkata Krishna Rao, B.; Pranothi, M.; Banda, S.; Kumar Bolla, P.; Kommineni, N. Stability characterization for pharmaceutical liposome product development with focus on regulatory considerations: An update. *International Journal of Pharmaceutics* **2022**, *624*, 122022. DOI: 10.1016/j.ijpharm.2022.122022.
- (3) Hashmi, M. P.; Koester, T. M. Applications of synthetically produced materials in clinical medicine. **2018**.
- (4) Guimarães, D.; Cavaco-Paulo, A.; Nogueira, E. Design of liposomes as drug delivery system for therapeutic applications. *Int J Pharm* **2021**, *601*, 120571. DOI: 10.1016/j.ijpharm.2021.120571.
- (5) (Luo, D.; Carter, K. A.; Miranda, D.; Lovell, J. F. Chemophototherapy: An Emerging Treatment Option for Solid Tumors. *Advanced Science* **2017**, *4* (1), 1600106. DOI: <https://doi.org/10.1002/advs.201600106>.
- (6) (1) Ghosh, S.; Sun, B.; Jahagirdar, D.; Luo, D.; Ortega, J.; Straubinger, R. M.; Lovell, J. F. Single-treatment tumor ablation with photodynamic liposomal irinotecan sucrosulfate. *Translational Oncology* **2022**, *19*, 101390. DOI: <https://doi.org/10.1016/j.tranon.2022.101390>.
- (7) McCall, J. G.; Kim, T. I.; Shin, G.; Huang, X.; Jung, Y. H.; Al-Hasani, R.; Omenetto, F. G.; Bruchas, M. R.; Rogers, J. A. Fabrication and application of flexible, multimodal light-emitting devices for wireless optogenetics. *Nat Protoc* **2013**, *8* (12), 2413-2428. DOI: 10.1038/nprot.2013.158.
- (8) Weinstain, R.; Slanina, T.; Kand, D.; Klán, P. Visible-to-NIR-Light Activated Release: From Small Molecules to Nanomaterials. *Chem Rev* **2020**, *120* (24), 13135-13272. DOI: 10.1021/acs.chemrev.0c00663.
- (9) Fomina, N.; Sankaranarayanan, J.; Almutairi, A. Photochemical mechanisms of light-triggered release from nanocarriers. *Advanced drug delivery reviews* **2012**, *64* (11), 1005-1020. DOI: <https://doi.org/10.1016/j.addr.2012.02.006>.
- (10) Katz, J. S.; Burdick, J. A. Light-Responsive Biomaterials: Development and Applications. *Macromolecular Bioscience* **2010**, *10* (4), 339-348. DOI: <https://doi.org/10.1002/mabi.200900297>.
- (11) Zhang, Z. Y.; Smith, B. D. Synthesis and characterization of NVOC-DOPE, a caged photoactivatable derivative of dioleoylphosphatidylethanolamine. *Bioconjugate chemistry* **1999**, *10* (6), 1150-1152. DOI: 10.1021/bc990087h.
- (12) Nagasaki, T.; Taniguchi, A.; Tamagaki, S. Photoenhancement of Transfection Efficiency Using Novel Cationic Lipids Having a Photocleavable Spacer. *Bioconjugate chemistry* **2003**, *14* (3), 513-516. DOI: 10.1021/bc0256603.
- (13) Chandra, B.; Mallik, S.; Srivastava, D. K. Design of photocleavable lipids and their application in liposomal "uncorking". *Chemical Communications* **2005**, (24), 3021-3023, 10.1039/B503423J. DOI: 10.1039/B503423J.

- (14) Chandra, B.; Subramaniam, R.; Mallik, S.; Srivastava, D. K. Formulation of photocleavable liposomes and the mechanism of their content release. *Organic & Biomolecular Chemistry* **2006**, *4* (9), 1730-1740, 10.1039/B518359F. DOI: 10.1039/B518359F.
- (15) Leung, S. J.; Romanowski, M. Light-activated content release from liposomes. *Theranostics* **2012**, *2* (10), 1020-1036. DOI: 10.7150/thno.4847.
- (16) Bayer, A. M.; Alam, S.; Mattern-Schain, S. I.; Best, M. D. Triggered Liposomal Release through a Synthetic Phosphatidylcholine Analogue Bearing a Photocleavable Moiety Embedded within the sn-2 Acyl Chain. *Chemistry – A European Journal* **2014**, *20* (12), 3350-3357. DOI: <https://doi.org/10.1002/chem.201304094>.
- (17) Chander, N.; Morstein, J.; Bolten, J. S.; Shemet, A.; Cullis, P. R.; Trauner, D.; Witzigmann, D. Optimized Photoactivatable Lipid Nanoparticles Enable Red Light Triggered Drug Release. *Small* **2021**, *17* (21), 2008198. DOI: <https://doi.org/10.1002/sml.202008198>.
- (18) Agasti, S. S.; Chompoosor, A.; You, C.-C.; Ghosh, P.; Kim, C. K.; Rotello, V. M. Photoregulated Release of Caged Anticancer Drugs from Gold Nanoparticles. *Journal of the American Chemical Society* **2009**, *131* (16), 5728-5729. DOI: 10.1021/ja900591t.
- (19) Vivero-Escoto, J. L.; Slowing, I. I.; Wu, C.-W.; Lin, V. S. Y. Photoinduced Intracellular Controlled Release Drug Delivery in Human Cells by Gold-Capped Mesoporous Silica Nanosphere. *Journal of the American Chemical Society* **2009**, *131* (10), 3462-3463. DOI: 10.1021/ja900025f.
- (20) Azagarsamy, M. A.; Alge, D. L.; Radhakrishnan, S. J.; Tibbitt, M. W.; Anseth, K. S. Photocontrolled Nanoparticles for On-Demand Release of Proteins. *Biomacromolecules* **2012**, *13* (8), 2219-2224. DOI: 10.1021/bm300646q.
- (21) Fournier, L.; Gauron, C.; Xu, L.; Aujard, I.; Le Saux, T.; Gagey-Eilstein, N.; Maurin, S.; Dubruille, S.; Baudin, J. B.; Bensimon, D.; et al. A blue-absorbing photolabile protecting group for in vivo chromatically orthogonal photoactivation. *ACS Chem Biol* **2013**, *8* (7), 1528-1536. DOI: 10.1021/cb400178m.
- (22) Olson, J. P.; Kwon, H.-B.; Takasaki, K. T.; Chiu, C. Q.; Higley, M. J.; Sabatini, B. L.; Ellis-Davies, G. C. R. Optically Selective Two-Photon Uncaging of Glutamate at 900 nm. *Journal of the American Chemical Society* **2013**, *135* (16), 5954-5957. DOI: 10.1021/ja4019379.
- (23) Lin, Q.; Yang, L.; Wang, Z.; Hua, Y.; Zhang, D.; Bao, B.; Bao, C.; Gong, X.; Zhu, L. Coumarin Photocaging Groups Modified with an Electron-Rich Styryl Moiety at the 3-Position: Long-Wavelength Excitation, Rapid Photolysis, and Photobleaching. *Angew Chem Int Ed Engl* **2018**, *57* (14), 3722-3726. DOI: 10.1002/anie.201800713.
- (24) Klausen, M.; Dubois, V.; Clermont, G.; Tonnelé, C.; Castet, F.; Blanchard-Desce, M. Dual-wavelength efficient two-photon photorelease of glycine by π -extended dipolar coumarins. *Chemical Science* **2019**, *10* (15), 4209-4219, 10.1039/C9SC00148D. DOI: 10.1039/C9SC00148D.
- (25) Chaud, J.; Morville, C.; Bolze, F.; Garnier, D.; Chassaing, S.; Blond, G.; Specht, A. Two-Photon Sensitive Coumarinyl Photoremovable Protecting Groups with Rigid Electron-Rich Cycles Obtained by Domino Reactions Initiated by a 5-exo-Dig Cyclocarbopalladation. *Organic Letters* **2021**, *23* (19), 7580-7585. DOI: 10.1021/acs.orglett.1c02778.
- (26) Agarwal, H. K.; Janicek, R.; Chi, S. H.; Perry, J. W.; Niggli, E.; Ellis-Davies, G. C. Calcium Uncaging with Visible Light. *J Am Chem Soc* **2016**, *138* (11), 3687-3693. DOI: 10.1021/jacs.5b11606.
- (27) Jakkampudi, S.; Abe, M.; Komori, N.; Takagi, R.; Furukawa, K.; Katan, C.; Sawada, W.; Takahashi, N.; Kasai, H. Design and Synthesis of a 4-Nitrobromobenzene Derivative Bearing an Ethylene Glycol Tetraacetic Acid Unit for a New Generation of Caged Calcium Compounds with Two-Photon Absorption Properties in the Near-IR Region and Their Application in Vivo. *ACS Omega* **2016**, *1* (2), 193-201. DOI: 10.1021/acsomega.6b00119.
- (28) Donato, L.; Mouro, A.; Davenport, C. M.; Herbivo, C.; Warther, D.; Léonard, J.; Bolze, F.; Nicoud, J.-F.; Kramer, R. H.; Goeldner, M.; et al. Water-Soluble, Donor-Acceptor Biphenyl Derivatives in the 2-(o-Nitrophenyl)propyl Series: Highly Efficient Two-Photon Uncaging of the Neurotransmitter γ -Aminobutyric Acid at $\lambda=800$ nm. *Angewandte Chemie International Edition* **2012**, *51* (8), 1840-1843. DOI: <https://doi.org/10.1002/anie.201106559>.
- (29) Pearson, S.; Feng, J.; del Campo, A. Lighting the Path: Light Delivery Strategies to Activate Photoresponsive Biomaterials In Vivo. *Advanced Functional Materials* **2021**, *31* (50), 2105989. DOI: <https://doi.org/10.1002/adfm.202105989>.

- (30) Morville, C.; Chaud, J.; Bolze, F.; Specht, A. Photolytical reactions for light induced biological effectors release: on the road to the phototherapeutic window. *Journal of Inclusion Phenomena and Macrocyclic Chemistry* **2021**, *101* (3), 291-304. DOI: 10.1007/s10847-021-01071-9.
- (31) Askes, S. H.; Bahreman, A.; Bonnet, S. Activation of a photodissociative ruthenium complex by triplet-triplet annihilation upconversion in liposomes. *Angew Chem Int Ed Engl* **2014**, *53* (4), 1029-1033. DOI: 10.1002/anie.201309389.
- (32) Huang, L.; Zhao, Y.; Zhang, H.; Huang, K.; Yang, J.; Han, G. Expanding Anti-Stokes Shifting in Triplet-Triplet Annihilation Upconversion for In Vivo Anticancer Prodrug Activation. *Angew Chem Int Ed Engl* **2017**, *56* (46), 14400-14404. DOI: 10.1002/anie.201704430.
- (33) Lv, W.; Long, K.; Yang, Y.; Chen, S.; Zhan, C.; Wang, W. A Red Light-Triggered Drug Release System Based on One-Photon Upconversion-Like Photolysis. *Adv Healthc Mater* **2020**, *9* (21), e2001118. DOI: 10.1002/adhm.202001118.
- (34) Huang, L.; Zeng, L.; Chen, Y.; Yu, N.; Wang, L.; Huang, K.; Zhao, Y.; Han, G. Long wavelength single photon like driven photolysis via triplet triplet annihilation. *Nat Commun* **2021**, *12* (1), 122. DOI: 10.1038/s41467-020-20326-6.
- (35) Brion, A.; Chaud, J.; Léonard, J.; Bolze, F.; Chassaing, S.; Frisch, B.; Heurtault, B.; Kichler, A.; Specht, A. Red Light-Responsive Upconverting Nanoparticles for Quantitative and Controlled Release of a Coumarin-Based Prodrug. *Advanced Healthcare Materials* **2023**, *12* (2), 2201474. DOI: <https://doi.org/10.1002/adhm.202201474>.
- (36) Liu, D. K. K.; Faulkner, L. R. P-Type delayed fluorescence from rubrene. *Journal of the American Chemical Society* **1977**, *99* (14), 4594-4599. DOI: 10.1021/ja00456a011.
- (37) Cheng, Y. Y.; Khoury, T.; Clady, R. G. C. R.; Tayebjee, M. J. Y.; Ekins-Daukes, N. J.; Crossley, M. J.; Schmidt, T. W. On the efficiency limit of triplet-triplet annihilation for photochemical upconversion. *Physical Chemistry Chemical Physics* **2010**, *12* (1), 66-71, 10.1039/B913243K. DOI: 10.1039/B913243K.
- (38) Cheng, Y. Y.; Fückel, B.; Khoury, T.; Clady, R. G.; Ekins-Daukes, N. J.; Crossley, M. J.; Schmidt, T. W. Entropically driven photochemical upconversion. *J Phys Chem A* **2011**, *115* (6), 1047-1053. DOI: 10.1021/jp108839g.
- (39) Askes, S. H. C.; Bonnet, S. Solving the oxygen sensitivity of sensitized photon upconversion in life science applications. *Nature Reviews Chemistry* **2018**, *2* (12), 437-452. DOI: 10.1038/s41570-018-0057-z.
- (40) Elamri, I.; Heumüller, M.; Herzig, L. M.; Stinal, E.; Wachtveitl, J.; Schuman, E. M.; Schwalbe, H. A New Photocaged Puromycin for an Efficient Labeling of Newly Translated Proteins in Living Neurons. *Chembiochem* **2018**, *19* (23), 2458-2464. DOI: 10.1002/cbic.201800408.
- (41) Spanedda, M. V.; Salomé, C.; Hilbold, B.; Berner, E.; Heurtault, B.; Fournel, S.; Frisch, B.; Bourel-Bonnet, L. Smart tools and orthogonal click-like reactions onto small unilamellar vesicles: Additional molecular data. *Data in Brief* **2015**, *5*, 145-154. DOI: <https://doi.org/10.1016/j.dib.2015.08.014>.
- (42) Salomé, C.; Spanedda, M. V.; Hilbold, B.; Berner, E.; Heurtault, B.; Fournel, S.; Frisch, B.; Bourel-Bonnet, L. Smart tools and orthogonal click-like reactions onto small unilamellar vesicles. *Chemistry and Physics of Lipids* **2015**, *188*, 27-36. DOI:10.1016/j.chemphyslip.2015.03.004.
- (43) Kulhánek, J.; Bureš, F.; Ludwig, M. Convenient methods for preparing π -conjugated linkers as building blocks for modular chemistry. *Beilstein Journal of Organic Chemistry* **2009**, *5*, 11. DOI: 10.3762/bjoc.5.11.
- (44) Li, C.; Koenigsmann, C.; Deng, F.; Hagstrom, A.; Schmuttenmaer, C. A.; Kim, J.-H. Photocurrent Enhancement from Solid-State Triplet-Triplet Annihilation Upconversion of Low-Intensity, Low-Energy Photons. *ACS Photonics* **2016**, *3* (5), 784-790. DOI: 10.1021/acsphotonics.5b00694.
- (45) Bernhardt, G.; Reile, H.; Birnböck, H.; Spruss, T.; Schönenberger, H. Standardized kinetic microassay to quantify differential chemosensitivity on the basis of proliferative activity. *J Cancer Res Clin Oncol* **1992**, *118* (1), 35-43. DOI: 10.1007/bf01192309.